agronomy

MDPI

Article

Photosystem II Repair Cycle in Faba Bean May Play a Role in Its Resistance to *Botrytis fabae* Infection

María Ángeles Castillejo [1,2,*], Ángel M. Villegas-Fernández [2], Tamara Hernández-Lao [1] and Diego Rubiales [2]

[1] Agroforestry and Plant Biochemistry, Proteomics and Systems Biology, Department of Biochemistry and Molecular Biology, University of Cordoba, UCO-CeiA3, 14014 Córdoba, Spain; b42helat@uco.es
[2] Institute for Sustainable Agriculture, Spanish National Research Council (CSIC), Avda. Menéndez Pidal, s/n, 14004 Córdoba, Spain; avillegas@ias.csic.es (Á.M.V.-F.); diego.rubiales@ias.csic.es (D.R.)
* Correspondence: bb2casam@uco.es

Abstract: Chocolate spot, which is caused by the necrotrophic fungus *Botrytis fabae*, is a major foliar disease occurring worldwide and dramatically reducing crop yields in faba bean (*Vicia faba*). Although chemical control of this disease is an option, it has serious economic and environmental drawbacks that make resistant cultivars a more sensible choice. The molecular mechanisms behind the defense against *B. fabae* are poorly understood. In this work, we studied the leave proteome in two faba bean genotypes that respond differently to *B. fabae* in order to expand the available knowledge on such mechanisms. For this purpose, we used two-dimensional gel electrophoresis (2DE) in combination with Matrix-Assisted Laser Desorption/Ionization (MALDI-TOF/TOF). Univariate statistical analysis of the gels revealed 194 differential protein spots, 102 of which were identified by mass spectrometry. Most of the spots belonged to proteins in the energy and primary metabolism, degradation, redox or response to stress functional groups. The MS results were validated with assays of protease activity in gels. Overall, they suggest that the two genotypes may respond to *B. fabae* with a different PSII protein repair cycle mechanism in the chloroplast. The differences in resistance to *B. fabae* may be the result of a metabolic imbalance in the susceptible genotype and of a more efficient chloroplast detoxification system in the resistant genotype at the early stages of infection.

Keywords: *Botrytis fabae*; faba bean; resistance; proteomic analysis; photosystem II repair cycle

Citation: Castillejo, M.Á.; Villegas-Fernández, Á.M.; Hernández-Lao, T.; Rubiales, D. Photosystem II Repair Cycle in Faba Bean May Play a Role in Its Resistance to *Botrytis fabae* Infection. *Agronomy* **2021**, *11*, 2247. https://doi.org/10.3390/agronomy11112247

Academic Editor: Giovanni Caruso

Received: 11 September 2021
Accepted: 3 November 2021
Published: 6 November 2021

1. Introduction

By virtue of its high nutritional value, faba bean (*Vicia faba* L.) is an important food legume for human consumption and livestock feeding [1]. In fact, it is regarded as an excellent protein crop on the basis of its ability to provide nitrogen inputs into temperate agricultural systems, and also because of its increased yield potential and nitrogen-fixing capacity relative to other grain legumes [2,3]. Faba bean is the fourth most widely grown cool season grain legume (pulse) globally after pea (*Pisum sativum*), chickpea (*Cicer arietinum*) and lentil (*Lens culinaris*) (FAOSTAT 2019; https://www.fao.org, accessed on 15 September 2021). However, its yield is greatly affected by some environmental conditions, including biotic and abiotic stresses [3,4].

The necrotrophic fungus *Botrytis fabae* Sard. (teleomorph: *Botryotinia fabae* Lu & Wu) causes chocolate spot, which is one of the most destructive diseases for faba bean plants worldwide [5,6]. Infected plants exhibit chocolate-colored lesions on aboveground parts and, especially, on leaves. The disease, which starts in bean crops where inoculum is present in residues from previous years or in contaminated seeds [7], may be especially aggressive under high humidity and temperature conditions. Such conditions can lead to extensive necrosis of plant tissues and severe damage, and can also favor the spread of the pathogen to other plants [8]. Prolonged favorable conditions for *B. fabae* growth can result in considerable economic crop losses through reduced grain yields and quality [9]. The

severity of chocolate spot epidemics can be mitigated with integrated disease management strategies, such as the use of clean seeds, crop rotations, lower planting densities, application of fungicides and selection of more resistant plant varieties [6,10]. Although some germplasm accessions have shown moderate to high levels of resistance [11], resistant cultivars adapted to different cultivation areas are scarcely available.

As a necrotrophic pathogen, *B. fabae* must kill and decompose host cells in order to feed on them. The fungus can infect plants via a variety of mechanisms mediated by lytic enzymes, toxins, stress-induced reactive oxygen species (ROS), necrosis-secreted proteins and a wide variety of secondary metabolites [12–16]. On the other hand, plants can stop the progression of the fungus by using constitutive or infection-induced mechanisms. Such mechanisms can be of the physical (cuticle and cell wall) [17,18] or chemical type (phytoanticipins and phytoalexins) [19], but can also involve induction of pathogenesis-related proteins or defensins, or accumulation of antimicrobial compounds [20,21].

Plants are known to accumulate ROS in response to necrotrophic fungi [22–27] and faba bean cultivars have been found to respond to *B. fabae* with differential ROS accumulation, lipid peroxidation and enzymatic ROS scavenging activity [28]. Recently, enhanced functionality in photosystem II (PSII), probably resulting from ROS accumulation in response to short-time exposure to *B. cinerea*, was reported in tomato plants [27]. However, little is known about the specific molecular mechanisms by which plants respond to *B. fabae*. A transcription factor (TF) analysis of the response of *M. truncatula* to *B. fabae* and *B. cinerea* [29] revealed some TFs to be involved in differential responses and others to be responsible for resistance to the two pathogens.

To our knowledge, few omics studies have focused on plant responses to *Botrytis*. As confirmed by using mutants at the transcriptomic level, *Arabidopsis thaliana* and tomato possess some genes whose expression is related to *B. cinerea* resistance. Such defense-related genes include some encoding PR protein 1 (PR1), β-1,3-glucanase and subtilisin-like protease, and other proteins involved in secondary metabolite synthesis (reviewed in [15]), but still others are involved in responses to abiotic stresses, such as signaling hormone pathways, which affect photosynthesis, and protein synthesis and transport [15,30,31]. Even fewer proteomics studies have addressed plant–*Botrytis* interactions [32,33] and most have focused on the pathogen *B. cinerea* (reviewed in [15]). Thus, Marra et al. used 2DE coupled to Matrix-Assisted Laser Desorption/Ionization (MALDI-TOF) analysis [32] to examine the interaction of beans with *B. cinerea* and *Trichoderma*. They found pathogenesis-related proteins and other disease-related factors, such as potential resistance genes, to be seemingly associated with interactions with both the pathogen and *Trichoderma*. In addition, a shotgun proteomic study of *B. cinerea*-infected tomato fruit at different ripening stages identified a substantial number of proteins responsible for pathogenicity (mainly PR and disease resistance proteins, proteases and peroxidases), as well as others protecting the fruit from the oxidative stress response by the host [33].

In the absence of a reference genome assembly for *Vicia faba* owing to its enormous size (13 Gbp) and complexity (e.g., abundance of transposable elements), high-throughput methods, such as transcriptome analysis, have proved efficient for enriching genomic resources (reviewed in [1]). However, only limited DNA sequence data from reported transcriptome datasets have been made available on public databases [34]. Using high-throughput omic technology can no doubt help expand existing knowledge of the plant–pathogen interaction and provide a basis for developing improved crop breeding programs. The main aim of this work was to go deeper into the knowledge of the molecular mechanisms underlying the defense against *B. fabae* in faba bean. For this purpose, we studied the leave proteome in two faba bean genotypes that respond differently to *B. fabae* by using two-dimensional gel electrophoresis (2DE) in combination with (MALDI-TOF/TOF) mass spectrometry (MS). Some results of the MS analysis were validated by assays of protease activity in gels. Overall, the results suggest that the key to stopping the spread of the pathogen onto leaves is mainly a regulatory ROS production mechanism occurring in the chloroplast.

2. Materials and Methods

2.1. Plant Material and Sample Collection

Two faba bean genotypes known to exhibit a contrasting response to *B. fabae* were used, namely: Baraca as susceptible genotype and BPL710 as resistant genotype [10,35]. Seeds of the two genotypes were grown in 1 L pots filled with a (1:1) sand–peat mixture under controlled conditions: (20 ± 2) °C, 12 h dark/12 h light photoperiod and a photon flux density of 150 µmol m^{-2} s^{-1}.

A total 27 plants per genotype were used, with leaves being sampled from 12 inoculated plants and 12 uninoculated (control) plants of each. Three other plants were inoculated and were used to score disease symptoms. Plants were inoculated according to Villegas-Fernandez et al. [35], with *B. fabae* local monosporic isolate (Bf-CO-05) being grown on Petri dishes containing V8 medium and spores suspended at a 4.5 × 10^5 spores/mL concentration in a glucose/water solution (1.2% *w*/*v*). Three-week-old plants were then sprayed with the suspension at a rate of 1.5 mL/plant and incubated in a growth chamber at a relative humidity above 95% in the dark. By contrast, control (uninoculated) plants were sprayed with a glucose solution containing no spores. Disease symptoms were evaluated after restoring the photoperiod 24 h later but keeping the relative humidity above 90%. Evaluations were done two and six days after inoculation (dai). Disease severity (DS) was calculated by visual estimation of the proportion of plant surface covered with chocolate spots, with estimates being corrected by increasing the weight of the aggressive lesions by 50% with the formula DS = (% nonaggressive lesions) + 1.5 × (% aggressive lesions). The results thus obtained were analyzed statistically with the software Statistix 8 (Analytical Software, Tallahassee, FL, USA). Data were subjected to the arcsin $\sqrt{x}$ transformation in order to offset evaluation bias and to increase normality in their distribution prior to analysis of variance (ANOVA).

Faba leaves for proteomic analyses were collected at two different times while both control and inoculated plants were still under incubation in the dark [35]. Sampling was done 6 h post-inoculation (hpi)—an early time at which no symptoms were apparent—and then 12 hpi—when the earliest symptoms of chocolate spots became macroscopically visible. All of the leaves from six individual plants (three biological replicates from two plants each) per condition (treatment and sampling time) were collected, frozen in liquid nitrogen and stored at −80 °C until protein extraction.

2.2. Protein Extraction and Gel Electrophoresis

Faba leaves samples (ca. 0.5 g fresh weight) from three independent replicates per treatment, sampling time and genotype were crushed with liquid nitrogen in a precooled mortar to obtain a fine powder. Proteins were extracted into TCA–phenol [36] and the resulting pellets were resuspended in a solubilization buffer containing 7 M urea (Merck, Kenilworth, NJ, USA), 2 M thiourea (Sigma–Aldrich, St. Louis, MI, USA), 2% (*w*/*v*) CHAPS (Sigma–Aldrich), 2% (*v*/*v*) Bio-Lyte 3–10 carrier ampholytes (BioRad, Hercules, CA, USA), 2% (*w*/*v*) DTT (Sigma–Aldrich) and Bromophenol Blue traces (Sigma–Aldrich). Protein concentrations were determined with the Bradford assay (BioRad) and proteins were then separated in 2D electrophoresis gels.

For 2DE analysis, 18-cm IPG DryStrips (Amersham Biosciences, Amersham, UK) were used with nonlinear pH gradients over the range 3–10. Strips were rehydrated passively for 6 h and then actively at 50 V for a further 6 h with 300 µL of sample buffer containing an amount of 400 µg of protein. Strips were loaded onto a PROTEAN IEF System (BioRad), focused at 20 °C with an increasing linear voltage and equilibrated according to Castillejo et al. [37]. They were then transferred onto vertical slabs of 10% SDS polyacrylamide gels. Electrophoresis runs were done at 30 V at 15 °C for 30 min, and then at 60 V for about 14 h until the dye front reached the bottom of the gel. The gels were loaded with broad-range molecular markers (Bio-Rad) and, after electrophoresis, stained with Coomassie Brilliant Blue G-250 [38].

2.3. Image Acquisition and Statistical Analysis

Gels were scanned with the Molecular imager FX ProPlus Multi-imager system (BioRad) and the images thus obtained (Supplementary Figure S1) were analyzed with the software PDQuest Advanced v. 8.0.1 (BioRad), using 10 times the background signal as the presence threshold for spots. The quantitative data gathered from the spots in each gel (viz., normalized spot volumes given as individual spot intensity/normalization factor) were used to designate differences when comparing gel images. A multivariate statistical analysis of the entire data set was performed by using the web-based software tool NIA array [39]. Those spots showing significant differences ($p \leq 0.05$) in intensity, exhibiting a minimum change of ± 2 and being consistently present among replicates were selected for further MS/MS analysis.

2.4. Protein Identification by Mass Spectrometry (MALDI-TOF/TOF)

Differential gel spots were excised for digestion with trypsin [40] and peptide fragments from digested proteins were analyzed by mass spectrometry. For that purpose, peptides were crystallized in an α-cyano-4-hydroxycinnamic acid matrix and subjected to MALDI-TOF/TOF analysis over the *m/z* range 800–4000 by using a 4800 Proteomics Analyzer (Applied Biosystems, Foster City, CA, USA) at an accelerating voltage of 20 kV. Spectra were internally calibrated against peptides from trypsin autolysis ($M + H^+ = 842.509$, $M + H^+ = 2211.104$) and the five most abundant peptide ions in each spectrum were used for fragmentation analysis to elucidate peptide sequences. A combined peptide mass fingerprinting (PMF)/tandem mass spectrometry (MS + MSMS) search was performed by using the software GPS Explorer™.5 (Applied Biosystems) over the nonredundant NCBInr database restricted to *Viridiplantae* taxonomy in combination with the MASCOT search engine (Matrix Science, London; http://www.matrixscience.com accessed on 15 September 2019). The following parameters were allowed: a minimum of two peptides matches and a single trypsin miscleavage, and peptide modifications by carbamidomethylcysteine and methionine oxidation. The maximum tolerance for peptide mass matching was limited to 20 ppm. The score level and a minimum of four peptides per protein were chosen as PMF confidence parameters. Proteins were characterized in functional terms against the NCBInr database (https://www.ncbi.nlm.nih.gov/guide/proteins/, accessed on 15 October 2021). In addition, BLAST analysis (tblastn) was performed for all the identified proteins using the reference transcriptome *Vicia faba RefTrans v2* (2017), with 37,378 sequences deposited in Pulse Crops Database (https://www.pulsedb.org/, accessed on 15 October 2021). Only matches with an expectation (E) value of $\leq 1 \times 10^{-6}$ were considered. Mass spectrometry analyses were conducted at the Proteomics Facility of the Central Research Support Service (SCAI) of the University of Córdoba (Spain).

2.5. Zymography

Proteins from leaves (200 mg of frozen powdered tissue) were extracted with a mixture of 200 mM TrisHCl at pH 7.4, 3% (*w*/*v*) insoluble polyvinylpolypyrrolidone (PVPP), 10% (*v*/*v*) glycerol, 5 mM diethiothreitol (DTT) and 0.25% (*v*/*v*) Triton X-100. Samples were allowed to stand on ice for at least 10 min and were then centrifuged at 16,000× *g* at 4 °C for 30 min, with the proteins present in the supernatant then being quantified with the Bradford assay [41].

SDS-PAGE slabs containing 0.1% gelatin and 9% acrylamide were analyzed according to Heussen and Dowdle [42]. Thus, samples containing 100 µg of protein were diluted with a nondenaturing Laemmli buffer [62.5 mM TrisHCl, 10% (*v*/*v*) glycerol, 0.001% (*w*/*v*) Bromophenol Blue] and loaded onto 1 mm thick gel slabs for electrophoresis at 50 V at 4 °C for 30 min, with the voltage being raised to 80 V until the front reached the end of the gel. The gels were loaded with Spectra Multicolor Broad Range Protein Ladder (Thermo Scientific). After electrophoresis, gels were incubated in 2.5% (*v*/*v*) Triton X-100 at room temperature under constant agitation for 30 min to remove SDS. They were then washed with distilled water three times to remove Triton X-100 and incubated in a proteolysis

buffer (100 mM citrate buffer, Na_2HPO_4/citric acid pH 6.8, 4 mM DTT and 10 mM cysteine) under constant agitation at 35 °C overnight. Proteolysis was stopped by transferring the gels to a solution containing 0.1% (*w*/*v*) Coomassie Brilliant Blue R-250 [43]. Finally, the gels were destained in a solution containing 40% methanol and 10% acetic acid until clear bands formed over a dark blue background.

3. Results

3.1. Disease Assessment

As can be seen in Figure 1, twelve hpi symptoms of *B. fabae* infection were already visible in the susceptible genotype (Baraca), but not in the resistant genotype (BPL710). Analyses of variance of the DS results revealed that the Baraca genotype was strongly affected both 2 and 6 dpi (average DS 23.9 and 52.5, respectively). On the other hand, the BPL710 genotype was highly resistant (ANOVA $p \leq 0.05$) in both samplings (average DS 11.6 and 14.6, respectively) (Figure 1; Supplementary Figure S2).

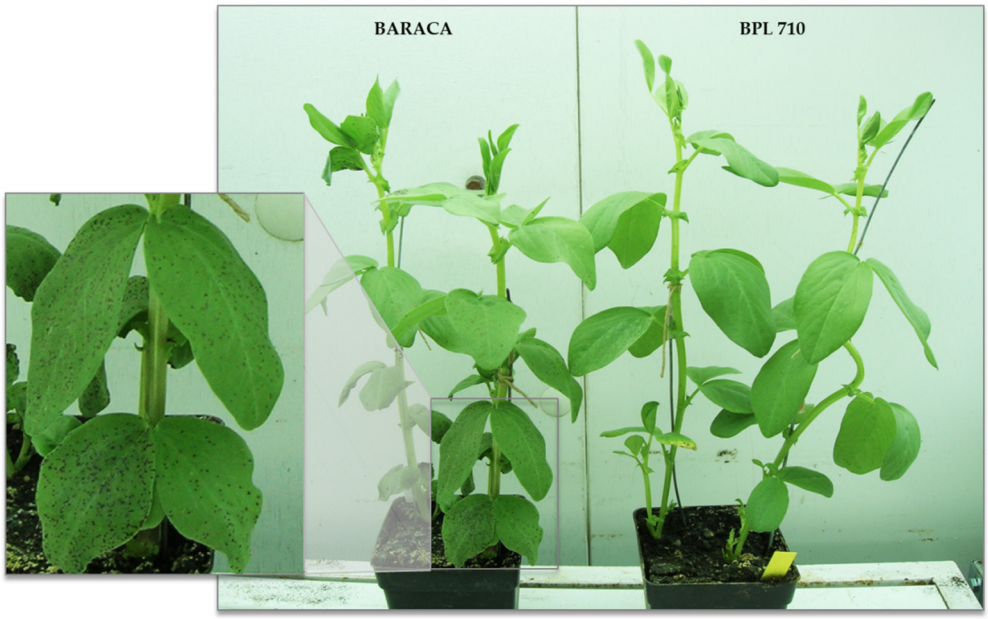

Figure 1. Contrasting response to *B. fabae* infection of three-week-old faba bean plants of Baraca (susceptible genotype) and BPL710 (resistant genotype) 12 h after inoculation.

3.2. Two-Dimensional Gel Electrophoresis and MSMS Analysis

Image analysis with the software PDQuest allowed, on average, 224 individual protein spots to be detected (Figure 2a; Supplementary Table S1). In addition, a hierarchical clustering analysis clearly separated the genotypes into two clusters (Figure 2b), thus confirming the reproducibility of the experiment. Principal component analysis (PCA) allowed 194 differential protein spots from the entire dataset to be identified by comparing genotypes (susceptible and resistant) and treatments (uninoculated and inoculated) in both samplings (6 and 12 hpi) (Figure 2c). The first two principal components (PCs) jointly explained 70% of the total variability in the data, PC1 separating genotypes. The PCs for individual genotypes explained 74% and 86% of variability in the susceptible and resistant genotype, respectively (Figure 2d,e). In both cases, samples clustered by sampling times.

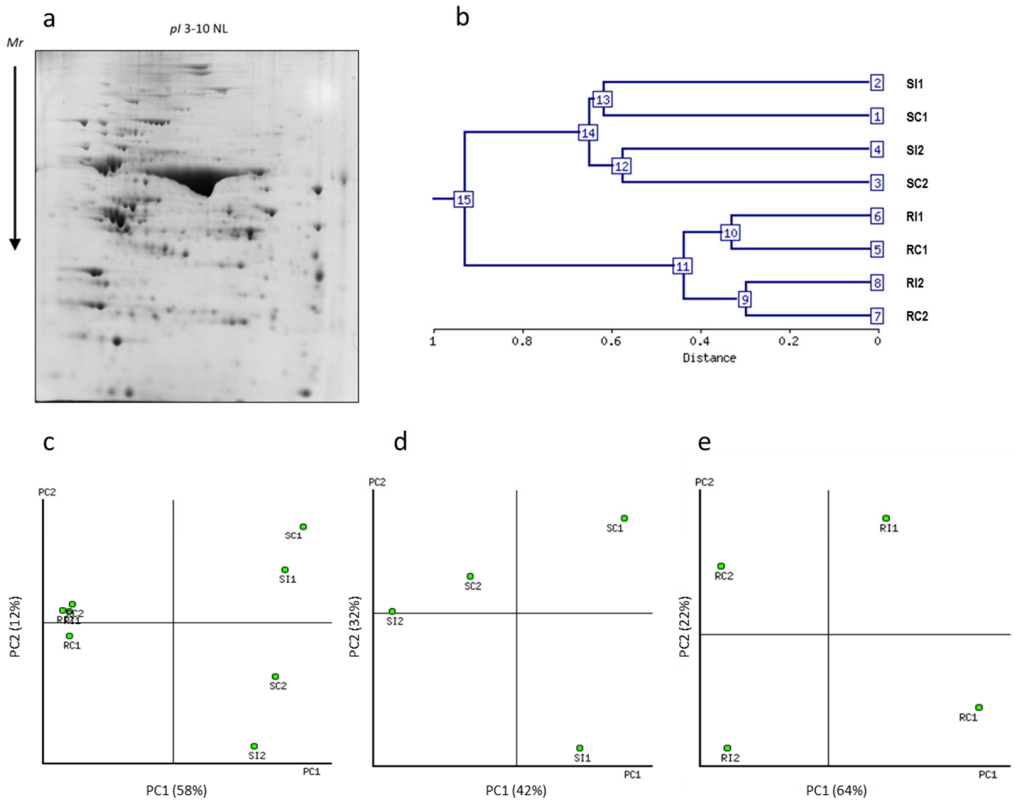

Figure 2. Typical Coomassie Brilliant Blue 2DE gel results for the susceptible genotype. (**a**) Dendrogram showing hierarchical clustering of experimental conditions. (**b**) Two-dimensional biplots showing associations between all experimental conditions in both genotypes (**c**), or independent genotypes (**d**,**e**), as generated by principal component analysis (PCA). Dendrogram and PCA data were obtained from average values under each set of experimental conditions: Susceptible (S) and resistant (R) genotypes; control (C) and *B. fabae* inoculated (I); 6 hpi (1) and 12 hpi (2).

Spots were classified as variable if they met the following criteria: (a) being consistently present or absent in the three replicates under each set of experimental conditions; (b) exhibiting at least a two-fold change in abundance ratio; and (c) exhibiting statistically significant differences ($p \leq 0.05$) between genotypes or treatments. A total of 129 protein spots were thus selected for MALDI-TOF/TOF analysis.

3.3. Protein Identification and Abundance Pattern Analysis

A protein search against the *Viridiplantae* index in the nonredundant NCBI database was performed and a total of 102 proteins were thus identified with high confidence (Table 1; Supplementary Figure S3), 70% of which matched legume species. Most of the proteins met the confidence identification criteria [viz., a score higher than 70 and at least four peptides per protein except for three spot proteins (viz., SSP 2802, 5002 and 11, which should be considered with caution)]. The proteins thus identified belonged to the main functional groups of energy and primary metabolism [photosynthesis (30) and other energy metabolism (6), carbohydrate (12) and amino acid metabolism (9)], followed by proteins of degradation (10), redox and response to stress groups (8) (Figure 3a).

Table 1. Proteins identified by MALDI-TOF MS analysis.

SSP [a]	Protein Name (% Identity to *V. faba* Transcriptome Entry) [b]	NCBI Accession	Score [c]	Species	PM [c]/ Coverage %	*Mr*/p*I* Experimental (Theoretical) [d]	Functional Category	More/Less Abundance Change Ratio (FDR) [e]					
								S1	S2	R1	R2	$\frac{R}{S}$ 1	$\frac{R}{S}$ 2
3504	Enolase (93.3% *Vf*_0033189)	gi|42521309	261	*Glycine max*	10/28	57.2/5.7 (48.0/5.3)	Carbohydrate met.	3.0	6.3	1.0	1.0	0.0	0.0
6302	Isocitrate dehydrogenase [NADP], chloroplastic (88.1% *Vf*_0028303)	gi|2497259	153	*Medicago sativa*	17/40	44.9/6.2 (48.7/6.2)	Carbohydrate met.	0.4	9.0	0.8	0.6	1.2	0.6
2204	Fructose-1,6-bisphosphatase (93.2% *Vf*_0032848)	gi|5305145	109	*Pisum sativum*	4/14	40.0/5.5 (36.3/6.3)	Carbohydrate met.	16.4	6.7	1.7	0.2	0.4	0.9
6203	Fructose-bisphosphate aldolase, cytoplasmic isozyme 1 (77.9% *Vf*_0020212)	gi|1168408	352	*Pisum sativum*	15/54	39.4/6.5 (38.7/6.4)	Carbohydrate met.	1.1	3.8	1.5	1.5	0.3	0.1
4104	Fructose-bisphosphate aldolase 2, chloroplastic (80.6% *Vf*_0020212)	gi|461501	183	*Pisum sativum*	10/37	38.4/5.8 (38.0/5.5)	Carbohydrate met.	0.6	1.2	27.6	0.2	0.5	1.6
5103	Fructose-bisphosphate aldolase 2, chloroplastic (80.6% *Vf*_0020212)	gi|461501	474	*Pisum sativum*	17/51	36.8/6.3 (38.0/5.5)	Carbohydrate met.	3.8	1.9	27.7	0.0	0.3	1.5
105	N-glyceraldehyde-2-phosphotransferase-like (84.2% *Vf*_0017868)	gi|8885622	133	*Arabidopsis thaliana*	7/22	33.4/5.2 (32.0/5.1)	Carbohydrate met.	6.4	0.8	0.5	1.0	0.2	0.0
1007	Triose-phosphate isomerase (75.1% *Vf*_0012679)	gi|15226479	205	*Arabidopsis thaliana*	9/25	29.5/5.6 (33.6/7.7)	Carbohydrate met.	3.6	2.3	1.1	1.2	0.5	0.2
2002	Triose-phosphate isomerase (75.1% *Vf*_0012679)	gi|15226479	292	*Arabidopsis thaliana*	11/29	29.1/5.8 (33.6/7.7)	Carbohydrate met.	10.4	5.1	1.9	1.1	0.5	0.2
3004	Triose-phosphate isomerase (89.1% *Vf*_0024793)	gi|57283985	165	*Phaseolus vulgaris*	7/31	21.9/5.6 (27.4/5.9)	Carbohydrate met.	2.2	4.7	1.0	0.4	0.0	1.6
2705	Phosphoglucomutase, cytoplasmic (97.9% *Vf*_0002214)	gi|12585296	109	*Pisum sativum*	10/8	74.3/5.6 (63.5/5.5)	Carbohydrate met.	9.5	0.0	1.0	1.0	0.0	0.0
3702	Phosphoglucomutase, cytoplasmic (97.9% *Vf*_0002214)	gi|12585296	222	*Pisum sativum*	10/23	70.8/5.7 (63.5/5.5)	Carbohydrate met.	6.3	19.0	0.4	0.9	2.3	8.8
603	Beta-amylase (88.5% *Vf*_0019893)	gi|3913031	149	*Medicago sativa*	7/17	61.3/5.0 (56.5/5.3)	Major CHO met.	3.1	8.2	1.0	0.5	1.0	1.6
4808	Methionine synthase/Cobalamin-independent synthase family protein (94.5% *Vf*_0005324)	gi|219522337	104	*Cicer arietinum*	12/19	92.8/5.9 (84.6/6.0)	Amino acid met.	6.9	190.5	1.5	0.7	3.4	20.1
5805	Methionine synthase/Cobalamin-independent synthase family protein (94.5% *Vf*_0005324)	gi|219522337	312	*Cicer arietinum*	15/26	93.2/6.0 (84.6/6.0)	Amino acid met.	20.8	50.3	0.5	0.7	5.2	4.0
5808	Methionine synthase/Cobalamin-independent synthase family protein (94.5% *Vf*_0005324)	gi|219522337	344	*Cicer arietinum*	20/31	92.2/6.1 (84.6/6.0)	Amino acid met.	3.2	25.4	0.3	2.3	3.9	1.0
2402	Alanine aminotransferase (82.2% *Vf*_0008300)	gi|29569153	140	*Oryza sativa*	8/17	54.1/5.6 (54.0/8.0)	Amino acid met.	8.1	17.6	0.7	2.9	2.4	0.8
3402	Alanine aminotransferase 2 (82.2% *Vf*_0008300)	gi|29569153	104	*Oryza sativa*	4/9	54.1/5.7 (54.0/8.0)	Amino acid met.	63.4	0.0	1.3	1.4	51.7	11.9
1402	5-enolpyruvylshikimate 3-phosphate synthase (79.5% *Vf*_0032499)	gi|55740769	73	*Camptotheca acuminate*	8/14	52.1/5.2 (56.1/8.2)	Amino acid met.	0.0	1.0	1.0	1.0	0.0	1.0
3613	Ketol-acid reductoisomerase chloroplastic (97.3% *Vf*_0004275)	gi|6225542	560	*Pisum sativum*	23/43	61.5/5.7 (63.2/6.6)	Amino acid met.	12.0	0.5	0.7	0.4	2.2	0.4
7501	Serine hydroxymethyltransferase 2 (91.7% *Vf*_0037308)	gi|222142531	203	*Glycine max*	13/29	57.1/6.9 (55.0/8.2)	Amino acid met.	2.1	1.7	1.6	1.0	0.3	0.0

Table 1. *Cont.*

SSP [a]	Protein Name (% Identity to *V. faba* Transcriptome Entry) [b]	NCBI Accession	Score [c]	Species	PM [c]/ Coverage %	*Mr*/*pI* Experimental (Theoretical) [d]	Functional Category	More/Less Abundance Change Ratio (FDR) [e]					
								S1	S2	R1	R2	$\frac{R}{S}$ 1	$\frac{R}{S}$ 2
1104	Putative lactoylglutathione lyase (78.0% *Vf*_0028431)	gi|15810219	183	*Arabidopsis thaliana*	8/26	33.4/5.3 (32.0/5.1)	Amino acid met.	3.7	1.2	0.6	0.4	0.5	0.4
7602	Chain A, Dihydrolipoamide Dehydrogenase (99.6% *Vf*_0005095)	gi|9955321	337	*Pisum sativum*	22/62	57.4/6.4 (50.0/6.1)	Lipid metabolism	51.2	25.1	0.9	0.8	7.7	1.9
2102	Pyruvate dehydrogenase E1 component subunit beta, mitochondrial (96.1% *Vf*_0005095)	gi|1709454	171	*Pisum sativum*	6/18	39.3/5.5 (39.0/5.9)	Lipid metabolism	0.7	6.7	1.0	1.0	0.0	0.0
3705	Zeaxanthin epoxidase, chloroplastic (72.1% *Vf*_0030326)	gi|5902706	92	*Solanum lycopersicum*	5/9	74.3/5.8 (73.6/6.2)	Hormone met.	1.0	1.0	0.6	1.1	∞	∞
5601	Polyphenol oxidase A1, chloroplastic (98.5% *Vf*_0006701)	gi|1172586	254	*Vicia faba*	8/8	64.9/6.0 (68.9/7.0)	Pigment biosynt.	0.0	1.0	1.0	1.0	0.0	1.0
5603	Polyphenol oxidase A1, chloroplastic (98.5% *Vf*_0006701)	gi|1172586	253	*Vicia faba*	9/13	64.7/6.0 (68.9/7.0)	Pigment biosynt.	9.5	0.0	1.0	1.0	0.0	0.0
4607	Polyphenol oxidase A1, chloroplastic (98.5% *Vf*_0006701)	gi|1172586	274	*Vicia faba*	9/12	64.4/5.9 (68.9/7.0)	Pigment biosynt.	1.0	1.0	0.0	1.0	∞	1.0
4605	Polyphenol oxidase A1, chloroplastic (98.5% *Vf*_0006701)	gi|1172586	151	*Vicia faba*	11/13	61.8/5.8 (68.9/7.0)	Pigment biosynt.	8.7	0.6	1.0	1.0	0.0	0.0
2103	Coproporphyrinogen-III oxidase, chloroplastic (70.9% *Vf*_0022525)	gi|2493810	148	*Nicotiana tabacum*	4/11	38.6/5.6 (45.3/7.6)	Co-factor and vitamine met.	7.7	1.2	1.0	1.0	0.0	0.0
2601	ATP synthase CF1 alpha subunit (96.7% *Vf*_0021629)	gi|219673973	546	*Trifolium subterraneum*	19/36	59.9/5.4 (55.7/5.1)	Energy metabolism	2.1	2.7	28.2	0.0	1.5	4.6
1601	ATP synthase CF1 alpha subunit (95.3% *Vf*_0021629)	gi|139387459	126	*Phaseolus vulgaris*	9/20	57.0/5.3 (55.7/5.2)	Energy metabolism	0.6	1.2	1.5	1.3	22.4	2.3
604	ATP synthase CF1 beta subunit ATP synthase alpha/beta family protein (97.6% *Vf*_0007913)	gi|295136979	572	*Pisum sativum*	18/48	58.9/5.2 (53.2/5.1)	Energy metabolism	0.7	2.7	1.0	1.6	9.0	2.3
505	ATP synthase CF1 beta subunit ATP synthase alpha/beta family protein (97.6% *Vf*_0007913)	gi|295136979	882	*Pisum sativum*	26/65	57.9/5.2 (53.2/5.1)	Energy metabolism	2.0	17.9	1.2	1.9	5.8	9.5
1503	ATP synthase CF1 alpha subunit (95.4% *Vf*_0021629)	gi|295137014	573	*Pisum sativum*	21/38	56.5/5.3 (54.7/5.7)	Energy metabolism	4.5	3.2	1.2	0.9	3.9	2.7
1501	ATP synthase CF1 beta subunit ATP synthase alpha/beta family protein (97.6% *Vf*_0007913)	gi|295136979	755	*Pisum sativum*	21/51	56.2/5.2 (53.2/5.1)	Energy metabolism	2.4	1.5	1.3	1.2	1.5	1.2
9701	Sulfite reductase (96.4% *Vf*_0029426)	gi|119225844	129	*Pisum sativum*	17/25	75.6/8.8 (77.3/9.1)	S metabolism	∞	1.0	1.0	1.0	1.0	1.0
3704	Transketolase (95.5% *Vf*_0028016)	gi|4586600	214	*Cicer arietinum*	3/30	82.8/5.8 (17.1/5.8)	Photosynthesis	11.3	7.0	1.2	1.0	35.9	3.2
3706	Transketolase (95.5% *Vf*_0028016)	gi|4586600	91	*Cicer arietinum*	4/44	82.7/5.8 (17.1/5.8)	Photosynthesis	4.0	4.0	1.0	0.5	18.0	2.8
4704	Transketolase (95.5% *Vf*_0028016)	gi|4586600	86	*Cicer arietinum*	4/44	82.5/5.9 (17.1/5.8)	Photosynthesis	3.8	17.1	0.6	0.7	6.4	1.7
4702	Transketolase (95.5% *Vf*_0028016)	gi|4586600	189	*Cicer arietinum*	5/48	81.6/5.8 (17.1/5.8)	Photosynthesis	3.8	3.1	1.0	1.1	8.1	1.5
1604	RuBisCO large subunit-binding protein subunit beta chloroplastic/chaperonin subunit beta (96.3% *Vf*_0035079)	gi|2506277	423	*Pisum sativum*	16/39	67.8/5.5 (63.3/5.8)	Photosynthesis	19.1	30.5	0.9	0.4	11.5	9.4
2602	RuBisCO large subunit-binding protein subunit beta chloroplastic/chaperonin subunit beta (96.3% *Vf*_0035079)	gi|2506277	72	*Pisum sativum*	11/27	66.8/5.6 (63.3/5.8)	Photosynthesis	1.8	2.4	2.2	0.5	1.9	1.5

Table 1. *Cont.*

SSP [a]	Protein Name (% Identity to *V. faba* Transcriptome Entry) [b]	NCBI Accession	Score [c]	Species	PM [c]/ Coverage %	*Mr*/p*I* Experimental (Theoretical) [d]	Functional Category	More/Less Abundance Change Ratio (FDR) [e]					
								S1	S2	R1	R2	$\frac{R}{S}$ 1	$\frac{R}{S}$ 2
1606	RuBisCO large subunit-binding protein subunit beta chloroplastic/chaperonin subunit beta (96.3% *Vf*_0035079)	gi|2506277	257	*Pisum sativum*	10/26	65.7/5.5 (63.3/5.8)	Photosynthesis	0.9	3.7	1.5	0.5	5.9	4.1
601	RuBisCO large subunit-binding protein subunit alpha chloroplastic /chaperonin-60alpha (98.4% *Vf*_0031659)	gi|1710807	480	*Pisum sativum*	19/36	65.8/5.0 (62.0/5.2)	Photosynthesis	2.4	5.2	0.7	0.2	1.0	3.3
4501	Ribulose-1,5-bisphosphate carboxylase/oxygenase large subunit (95.9% *Vf*_0007913)	gi|825737	556	*Carya illinoinensis*	20/40	57.1/5.8 (51.6/6.1)	Photosynthesis	26.5	7.5	0.5	37.7	4.3	2.8
4505	Ribulose-1,5-bisphosphate carboxylase/oxygenase large subunit (96.5% *Vf*_0007913)	gi|33113311	584	*Carya ovate*	23/42	55.8/5.9 (51.4/6.1)	Photosynthesis	5.1	1.7	6.2	1.4	41.3	3.3
4406	Ribulose-1,5-bisphosphate carboxylase/oxygenase large subunit (95.6% *Vf*_0007913)	gi|21634071	485	*Cressa depressa*	23/44	55.5/5.8 (50.6/6.7)	Photosynthesis	3.3	4.3	0.1	17.6	38.4	17.3
5507	Ribulose-1,5-bisphosphate carboxylase/oxygenase large subunit (96.4% *Vf*_0007913)	gi|225544093	709	*Caragana camilli-schneideri*	25/45	54.4/6.0 (52.8/6.3)	Photosynthesis	1.9	1.4	0.8	2.4	41.8	2.0
5408	Ribulose-1,5-bisphosphate carboxylase/ oxygenase (95.7% *Vf*_0007913)	gi|74179244	619	*Aristolochia arborea*	23/44	52.5/6.1 (52.0/6.1)	Photosynthesis	14.6	1.3	0.9	0.7	21.7	7.2
5407	Ribulose-1,5-bisphosphate carboxylase/ oxygenase large subunit (95.3% *Vf*_0007913)	gi|62861204	759	*Paracroton zeylanicus*	25/50	50.8/6.2 (52.0/6.0)	Photosynthesis	14.1	0.9	0.6	0.9	11.2	3.7
2304	Phosphoglycerate kinase chloroplastic (86.1% *Vf*_0006851)	gi|129915	192	*Triticum aestivum*	9/19	49.6/5.6 (50.0/6.6)	Photosynthesis	96.2	2.6	1.0	1.0	0.0	0.0
2301	Phosphoglycerate kinase chloroplastic (86.1% *Vf*_0006851)	gi|129915	254	*Triticum aestivum*	7/16	46.1/5.6 (50.0/6.6)	Photosynthesis	12.8	3.9	6.9	0.8	6.3	4.6
2303	Phosphoglycerate kinase chloroplastic (85.6% *Vf*_0006851)	gi|2499497	571	*Nicotiana tabacum*	15/33	44.5/5.6 (50.3/8.5)	Photosynthesis	3.2	3.7	2.5	1.5	3.7	1.7
7503	Ribulose-1,5-bisphosphate carboxylase/ oxygenase large (95.9% *Vf*_0007913)	gi|825737	372	*Carya illinoinensis*	21/42	56.2/6.7 (51.6/6.1)	Photosynthesis	3.5	6.8	0.9	1.8	98.3	3.2
6418	Ribulose-1,5-bisphosphate carboxylase/ oxygenase (95.7% *Vf*_0007913)	gi|74179244	589	*Aristolochia arborea*	24/42	53.7/6.3 (52.0/6.1)	Photosynthesis	15.2	1.7	0.8	1.4	1.3	2.5
8308	Geranylgeranyl hydrogenase (91.3% *Vf*_0032793)	gi|19749359	267	*Glycine max*	18/38	48.6/8.7 (51.7/9.1)	Photosynthesis	1.7	5.0	0.9	0.4	2.1	5.9
203	Sedoheptulose-1,7-bisphosphatase (81.8% *Vf*_0007079)	gi|229597543	230	*Cucumis sativus*	9/21	42.8/5.2 (42.5/5.9)	Photosynthesis	2.4	3.2	1.0	0.7	1.6	1.4
3202	Sedoheptulose-1,7-bisphosphatase (81.8% *Vf*_0007079)	gi|229597543	215	*Cucumis sativus*	12/34	42.6/5.6 (42.5/5.9)	Photosynthesis	5.5	11.2	1.5	3.3	1.7	1.5
1204	Phosphoribulokinase (99.1% *Vf*_0003052)	gi|1885326	350	*Pisum sativum*	14/46	41.4/5.4 (39.2/5.4)	Photosynthesis	2.4	2.5	4.8	0.9	2.3	2.7

Table 1. *Cont.*

SSP [a]	Protein Name (% Identity to *V. faba* Transcriptome Entry) [b]	NCBI Accession	Score [c]	Species	PM [c]/ Coverage %	*Mr*/p*I* Experimental (Theoretical) [d]	Functional Category	More/Less Abundance Change Ratio (FDR) [e]					
								S1	S2	R1	R2	$\frac{R}{S}$ 1	$\frac{R}{S}$ 2
2202	Phosphoribulokinase (99.1% _0003052)	gi|1885326	160	*Pisum sativum*	7/27	41.1/5.5 (39.2/5.4)	Photosynthesis	1.2	1.5	1.2	0.8	3.4	2.0
1201	Photosystem II stability/assembly factor HCF136, chloroplast precursor (78.8% *Vf*_0033934)	gi|255559812	237	*Ricinus communis*	8/20	41.1/5.3 (43.4/7.1)	Photosynthesis	1.3	2.2	1.8	2.0	0.5	0.3
3107	Aldolase (80.8% *Vf*_0017749)	gi|169039	137	*Pisum sativum*	9/27	38.5/5.6 (38.0/5.5)	Photosynthesis	2.3	1.6	5.3	1.2	0.3	1.7
3105	Aldolase (80.8% *Vf*_0017749)	gi|169039	88	*Pisum sativum*	8/29	38.0/5.6 (38.0/5.5)	Photosynthesis	0.0	0.1	∞	0.8	0.0	0.1
1001	Chloroplast chlorophyll a/b binding protein (99.2% *Vf*_0037012)	gi|157786302	265	*Pisum sativum*	10/34	30.3/5.2 (28.4/5.5)	Photosynthesis	0.9	0.8	6.8	0.9	0.3	1.4
4306	Transaminase mtnE, putative (80.9% *Vf*_0021772)	gi|255562088	159	*Ricinus communis*	5/11	46.2/5.9 (50.9/6.9)	Photosynthesis	1.2	4.4	1.0	1.0	0.0	0.0
401	Chloroplast ribulose-1,5-bisphosphate carboxylase activase (81.0% *Vf*_0005564)	gi|115392208	122	*Triticum aestivum*	6/21	51.7/5.1 (40.3/6.5)	Photosynthesis	0.9	0.0	1.0	1.0	0.0	0.0
1502	UDP-glucose pyrophosphorylase (89.7% *Vf*_0034269)	gi|12585472	271	*Astragalus penduliflorus*	12/29	54.1/5.3 (51.6/5.9)	Protein synthesis	1.1	2.3	1.0	1.0	0.0	0.0
2801	ClpC protease (92.1% *Vf*_0007069)	gi|4105131	70	*Spinacia oleracea*	12/16	96.6/5.6 (99.6/8.8)	Protein degrad.	6.7	8.8	0.5	0.4	8.9	2.7
2804	ClpC protease (98.5% *Vf*_0007069)	gi|461753	145	*Pisum sativum*	19/26	96.1/5.6 (102.8/6.6)	Protein degrad.	5.3	1.6	0.3	1.4	20.0	1.2
1802	ATP-dependent Clp protease (98.5% *Vf*_0007069)	gi|461753	383	*Pisum sativum*	26/33	95.3/5.3 (102.8/6.6)	Protein degrad.	2.3	6.4	1.5	1.2	1.1	1.7
2703	Cell division protease ftsH homolog, chloroplastic (91.1% *Vf*_0034616)	gi|17865463	262	*Medicago sativa*	16/30	75.4/5.6 (75.8/5.6)	Protein degrad.	5.9	7.0	1.1	1.6	0.9	0.2
2707	Cell division protease ftsH homolog chloroplastic (91.1% *Vf*_0034616)	gi|17865463	140	*Medicago sativa*	10/19	74.8/5.7 (75.8/5.6)	Protein degrad.	14.1	60.9	0.6	0.8	4.0	3.5
2706	Cell division protease ftsH homolog, chloroplastic (91.1% *Vf*_0034616)	gi|17865463	315	*Medicago sativa*	21/38	70.9/5.7 (75.8/5.6)	Protein degrad.	2.9	6.0	0.6	1.2	2.7	0.9
1702	Putative zinc dependent protease/FTSH protease 8 (87.0% *Vf*_0002195)	gi|84468324	206	*Trifolium pretense*	11/22	74.5/5.3 (75.4/5.5)	Protein degrad.	∞	8.0	0.7	1.6	∞	1.2
2101	Serine-type endopeptidase (96.5% *Vf*_0035526)	gi|270342123	70	*Phaseolus vulgaris*	5/15	39.5/5.4 (45.2/7.7)	Protein degrad.	∞	1.0	1.0	1.0	1.0	1.0
2802	Ubiquitin-specific-processing protease 8 (62.7% *Vf*_0023012)	gi|257050978	61	*Arabidopsis thaliana*	13/27	99.1/5.2 (90.7/5.5)	Protein degrad.	1.0	10.4	1.0	1.0	1.0	0.0
3803	ATP-dependent Clp protease/CLPC homologue 1 (98.5% *Vf*_0007069)	gi|461753	308	*Pisum sativum*	19/26	83.8/5.7 (102.8/6.6)	Protein degrad.	7.3	13.4	1.7	1.6	8.2	3.0
702	Chaperone DnaK (stromal 70 kDa heat shock-related protein, chloroplastic) (93.7% *Vf*_0024557)	gi|92870233	955	*Medicago truncatula*	27/38	81.5/5.0 (75.8/5.2)	Stress response	3.5	4.5	1.6	0.6	4.2	3.0
1701	Heat shock protein 70 (92.1% *Vf*_0006213)	gi|56554972	562	*Medicago sativa*	23/40	81.8/5.3 (71.4/5.1)	Stress response	3.6	4.5	2.1	0.8	1.7	5.3
2701	Heat shock 70 kDa protein mitochondrial (93.1% *Vf*_0016658)	gi|585272	216	*Pisum sativum*	14/26	76.2/5.6 (72.4/5.8)	Stress response	13.1	11.1	1.0	1.0	0.0	0.0
4302	Monodehydroascorbate reductase I (92.0% *Vf*_0006284)	gi|51860738	167	*Pisum sativum*	10/24	47.9/5.8 (47.4/5.8)	Stress response	3.7	2.2	6.4	1.0	1.4	0.3
3001	L-ascorbate peroxidase, cytosolic (60.9% *Vf*_0035596)	gi|1351963	171	*Pisum sativum*	8/34	31.0/6.1 (27.2/5.5)	Stress response	1.9	0.5	1.1	0.6	0.5	2.1

Table 1. *Cont.*

SSP [a]	Protein Name (% Identity to *V. faba* Transcriptome Entry) [b]	NCBI Accession	Score [c]	Species	PM [c]/ Coverage %	*Mr*/p*I* Experimental (Theoretical) [d]	Functional Category	More/Less Abundance Change Ratio (FDR) [e]					
								S1	S2	R1	R2	$\frac{R}{S}$ 1	$\frac{R}{S}$ 2
3103	CDSP32 protein (Chloroplast Drought-induced Stress Protein of 32 kDa) (69.4% *Vf*_0033087)	gi|2582822	133	*Solanum tuberosum*	4/14	33.8/6.0 (33.8/8.1)	Stress response	0.9	0.8	0.3	0.2	0.4	0.7
1206	NADPH-dependent alkenal/one oxidoreductase, chloroplastic (85.3% *Vf*_0022282)	XP_003532009.1	190	*Glycine max*	6/28	40.6/5.4 (31.2/9.2)	Redox	1.0	1.0	1.0	∞	1.0	1.0
11	Thioredoxin peroxidase (80.1% *Vf*_0034677)	gi|21912927	108	*Nicotiana tabacum*	3/16	21.6/5.2 (30.1/8.2)	Redox	2.4	0.3	16.3	0.6	0.0	0.7
5305	GDP-D-Mannose 3′,5′-Epimerase (90.2% *Vf*_0021019)	gi|15241945	108	*Arabidopsis thaliana*	8/26	49.6/6.0 (43.1/5.8)	Cell wall	8.0	19.0	1.0	1.0	0.0	0.0
502	Hydroxyproline-rich glycoprotein family protein	gi|18411523	147	*Arabidopsis thaliana*	9/13	60.7/4.8 (49.4/5.2)	Cell wall	3.8	2.0	0.8	0.7	0.8	0.6
4404	Gdp-Mannose-3′, 5′-Epimerase (89.9% *Vf*_0021019)	gi|83754656	112	*Arabidopsis thaliana*	9/22	50.6/5.9 (43.2/5.8)	Cell wall	0.5	3.7	1.0	1.0	0.0	0.0
101	PAP fibrillin (84.1% *Vf*_0025094)	gi|87240799	268	*Medicago truncatula*	8/18	34.4/4.9 (34.1/4.9)	Cell organization	1.4	1.7	1.8	0.5	0.2	1.5
1308	Actin (99.7% *Vf*_0005527)	gi|34541966	560	*Trifolium pretense*	16/51	47.9/5.5 (41.9/5.3)	Cell organization	0.7	12.9	0.4	7.7	3.1	0.5
1404	Actin (99.1% *Vf*_0028038)	gi|1498334	113	*Glycine max*	8/39	49.3/5.3 (37.3/5.5)	Cell organization	2.6	11.5	1.0	1.0	0.0	0.0
1304	Actin (99.7% *Vf*_0005527)	gi|34541966	431	*Trifolium pretense*	16/53	49.0/5.3 (41.9/5.3)	Cell organization	0.8	8.7	1.0	1.8	0.5	0.6
3205	Actin (94.3% *Vf*_0008358)	gi|1498384	172	*Zea mays*	5/19	39.7/5.6 (37.3/5.5)	Cell organization	0.0	6.4	1.0	1.0	0.0	0.0
3302	Elongation factor Tu (97.5% *Vf*_0005994)	gi|6015084	284	*Pisum sativum*	17/35	48.1/5.6 (53.1/6.6)	Transcription/ Translation	∞	2.8	2.5	1.2	∞	0.8
3309	Elongation factor Tu (97.5% *Vf*_0005994)	gi|6015084	480	*Pisum sativum*	22/43	47.9/5.7 (53.1/6.6)	Transcription/ Translation	0.3	13.0	11.7	2.2	1.7	1.4
3307	Elongation factor Tu (97.5% *Vf*_0005994)	gi|6015084	584	*Pisum sativum*	22/46	47.7/5.7 (53.1/6.6)	Transcription/ Translation	7.6	7.5	1.0	0.9	11.6	8.2
9401	Elongation factor 1 alpha (96.9% *Vf*_0022300)	gi|61741088	201	*Actinidia deliciosa*	16/37	54.0/9.0 (49.6/9.2)	Transcription/ Translation	4.4	4.8	1.3	2.4	7.0	4.9
3603	Tic62 protein (89.8% *Vf*_0007594)	gi|21616072	99	*Pisum sativum*	7/24	61.8/5.7 (57.1/8.8)	Signaling	1.0	0.0	1.0	1.0	1.0	0.0
1708	V-type proton ATPase catalytic subunit A (95.9% *Vf*_0002956)	gi|12585490	146	*Citrus unshiu*	17/42	74.4/5.5 (68.9/5.3)	Transport	8.9	54.4	0.7	1.2	3.8	5.3
5002	Carbonate dehydratase (64.2% *Vf*_0022150)	gi|47606728	105	*Flaveria bidentis*	3/17	30.3/6.2 (35.9/5.8)	Miscellaneous	1.3	5.8	1.3	0.6	0.5	3.1
6003	Carbonic anhydrase (85.8% *Vf*_0022150)	gi|270342124	153	*Phaseolus vulgaris*	7/34	29.0/6.5 (35.9/8.1)	Miscellaneous	0.9	0.5	3.3	∞	0.2	0.0

[a] Standard spot number assigned to each spot protein (SSP) by PDQuest software (BioRad). [b] Percentages of identity to *V. faba* transcriptome entries [*Vicia faba RefTrans V2* (2017) (https://www.pulsedb.org/, accessed on 15 October 2021)] obtained by Blast (tblastn) analysis are displayed in brackets. The coding "v.faba_CSFL_reftransV2_number" has been simplified by "*Vf*_number" for each transcript. [c] PM: number of peptides matched (from peptide mass fingerprinting) with the homologous protein from the database. Some of these peptides were automatically MSMS fragmented. [d] Experimental mass (Mr, kDa) and pI were calculated with PDQuest software and standard molecular mass markers. Theoretical values were retrieved from the protein database (NCBInr). [e] Values are given as normalized volume (calculated with PDQuest software) and represent change ratios in response to *B. fabae* inoculation of each genotype (S: Baraca; R: BPL710), and between uninoculated genotypes (R/S) at both sampling times (1: 6 hpi; 2: 12 hpi).

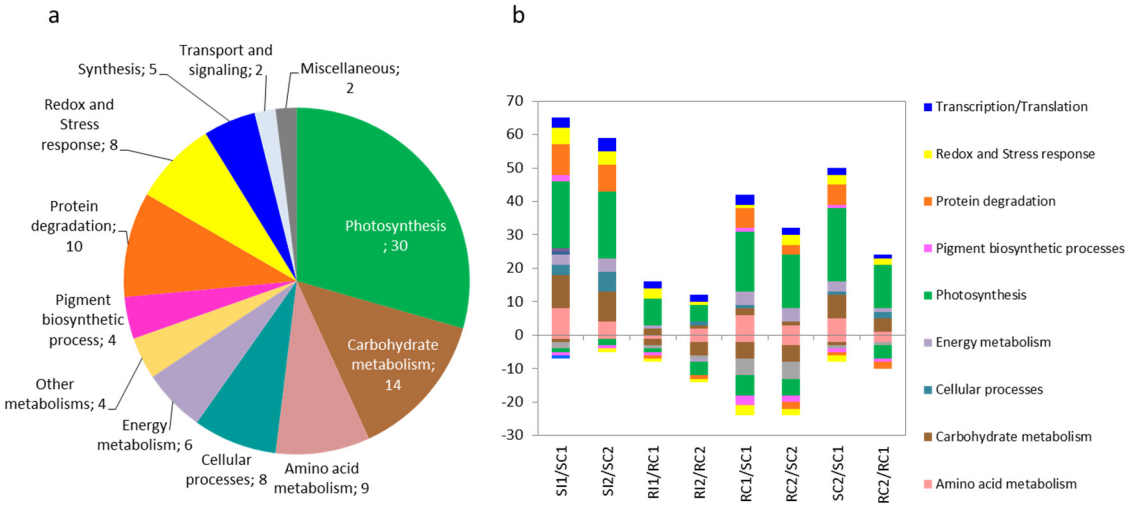

Figure 3. Functional groups of differential proteins. (**a**) Proteins up- or down-accumulating in response to *B. fabae* inoculation as grouped by functional category. (**b**) Susceptible (S) and resistant (R) genotype; control (C) and *B. fabae* inoculated (I); 6 hpi (1) and 12 hpi (2).

Figure 3b compares treatments, genotypes and sampling times. The susceptible genotype (S) showed the largest number of changes in proteins in response to inoculation, but mainly in those of the primary and energy metabolism groups (Figure 3b). In fact, a strikingly large number of degradation proteins showed changes in S genotype in response to inoculation that were not observed in the resistant genotype (R). The group of degradation proteins comprised ten proteases, namely: three cell division proteases ftsH chloroplastic (gi | 17865463), two ATP-dependent Clp proteases (gi | 461753), two Clp proteases (gi | 4105131, gi | 461753), one ubiquitin-specific protease 5 (gi | 257050978), one zinc dependent protease/FTSH protease 8 (gi | 84468324) and one serine-type endopeptidase (gi | 270342123). Interestingly, most of the identified proteases were significantly increased in response to inoculation in the susceptible genotype but, as revealed by the heat map (Figure 4a, Table 1), none was in the resistant genotype. A comparison of the uninoculated leaf proteome revealed a much greater number of proteins of the energy metabolism and protein degradation groups in R than in S, mainly in the first sampling (Figures 3b and 4a). In addition, these functional groups were increased in control S plants in the second sampling.

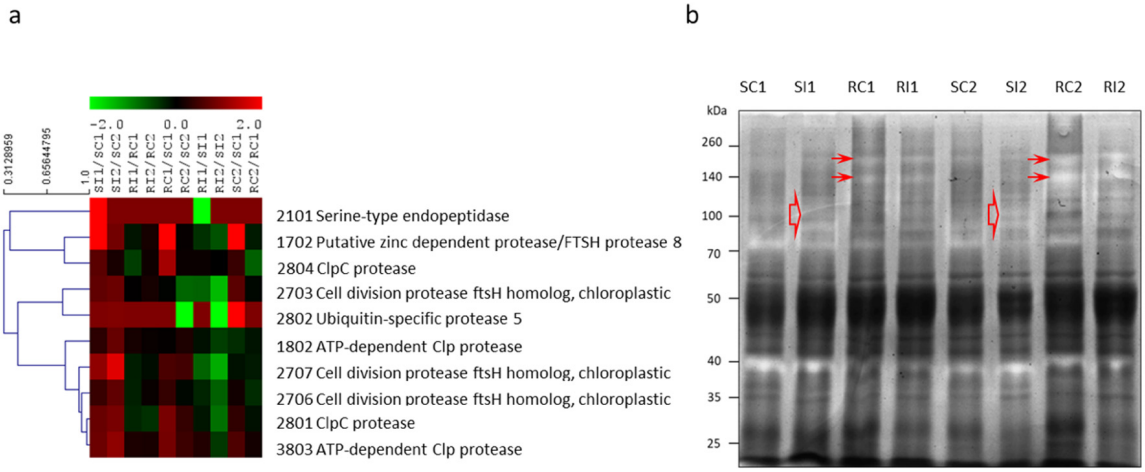

Figure 4. (**a**) Hierarchical clustering of proteases identified by MALDI-TOF analysis based on protein abundance as determined by 2DE. Susceptible genotype (S) and resistant genotype (R); control (C) and *B. fabae* inoculated (I); 6 hpi (1) and 12 hpi (2). (**b**) Zymogram of proteases in faba leaves separated by SDS-PAGE bearing gelatin under nondenaturing conditions. Arrowheads denote differential bands between genotypes or treatments.

3.4. Protease Gel Activity

The results of the protease gel activity assay confirmed those previously obtained by MS. Protease bands corresponding to high molecular weights (~90 to 120 kDa) were stronger in inoculated plants of the susceptible genotype in both samplings, coinciding with the molecular weight of some proteases identified by MALDI-TOF (viz., Clp proteases, SSPs 1802, 2801, 2804, 3803; and Ubiquitin-specific-processing protease 8, SSP 2802) (Figure 4b; Supplementary Figure S4). Gel activity assay also exposed a strong band at 40 kDa not changing substantially with the specific conditions and potentially corresponded to the serine-type endopeptidase identified by MS analysis (SSP 2101). In any case, the most striking result was the presence of two well-defined protease bands at high molecular weights (140–250 kDa) that were especially strong in the resistant genotype (and, particularly, in the second sampling). The area of the protease activity bands were estimated using ImageJ software (ImageJ.JS (imjoy.io)), and the data are presented in Supplemental Figure S5. Since activity gels were used under native conditions and 2DE-MS analyses conducted under denaturing conditions, these bands may well correspond to protein complexes not identified with the denaturing gels.

4. Discussion

Botrytis fabae is a necrotrophic plant pathogen causing chocolate spot, which is one of the most devastating diseases for faba bean production worldwide [5,6]. The mechanism by which plants counteract infection by this pathogen is of great agronomic interest. ROS production (especially H_2O_2 induction by *Botrytis*) is known to occur in a wide variety of plants [23,25–27] and to be one of the earliest plant responses to fungal infection [22,24]. *Botrytis fabae* reportedly increases lipid peroxidation, and the levels of ROS and antioxidant enzymes (superoxide dismutase, catalase and ascorbate peroxidase), substantially in faba bean [28]. In fact, ROS were found to accumulate rapidly in leaf tissue of a resistant cultivar at early stages of infection, but more markedly and over longer periods at later stages in its susceptible counterpart [28].

4.1. The Role of Chloroplasts as Redox Sensors Eliciting an Acclimatory Response to Stressing Conditions

ROS accumulation at an early stage of infection is triggered by plasma membrane-bound NADPH oxidases and typically occurs in the apoplast [44]. However, chloroplastic and peroxisomal ROS production have been reported to contribute to plant immunity as well [45,46]. Although ROS can also be produced by other organelles (notably peroxisomes and mitochondria), the chloroplast is possibly a major source. Some proteins in the chloroplast are involved in cross-talk with the cytosol and nucleus to govern the outcome of defense signaling [47]. Besides triggering ROS signals, chloroplasts can perceive, mediate or even amplify ROS signals originating in the apoplast [48]. In addition, there is evidence that the role of chloroplastic ROS production in coordinating cell death or modulating defense outputs is highly specific in targeting various types of invading pathogens. Thus, some chloroplastic components may be specific targets for microbial effector molecules, which suggest that chloroplasts communicate through these target molecules to elicit ROS production in the apoplast, presumably to contain spread of the lesion [49].

Chloroplast-derived ROS has been shown to play a role in plant resistance against *B. cinerea* [27,50]. Thus, histochemical analysis revealed ROS accumulation in tomato leaves 24 h after application of *B. cinerea* spores. A defense response accompanied by an improvement in photosystem II (PSII), possibly triggered by ROS upon short-time exposure, was observed. However, the relatively increased time of exposure to these molecules made them harmful to PSII functionality [27,51]. In addition, H_2O_2 levels in strawberry leaves were found to correlate positively with disease severity, and to be influenced by both leaf age and light quality [52].

Through photosynthesis, chloroplasts play a central role as redox sensors of environmental conditions by eliciting acclimatory or stress-defense responses [53,54]. In chloro-

plasts, chaperone systems refold proteins after stress, while proteases degrade misfolded and aggregated proteins that cannot be refolded [55]. A study on *Arabidopsis thaliana* demonstrated a major role of Hsp70 chaperones and Clp proteases in the folding and degradation of misfolded or damaged proteins under variable stress conditions in the chloroplast [55]. Caseinolytic proteases (Clps) function as molecular chaperones and confer thermotolerance to plants. The results of a differential gene expression analysis of Clps in wheat suggest a potential role in cold, salt and biotic stresses, and confirm the previously reported role in thermotolerance [56]. ClpATPases class I (ClpB/HSP100 and ClpC) function in assembly and disassembly with protein complexes, acting together with the HSP70/DnaK chaperone system to remodel denatured protein aggregates [57]. On the other hand, plant ClpC proteins act as stromal molecular chaperones in importing and protecting unfolded newly synthesized proteins, which are responsible for maintaining homeostasis [58–61].

In the present work two ATP-dependent Clp, two ClpC proteases and three Hsp70 (one as Chaperone DnaK) were found to be considerably increased in the susceptible genotype in response to inoculation. This result suggests that the chloroplast may respond to *B. fabae* inoculation by triggering a mechanism to repair damaged proteins. The previous proteins were highly represented at the constitutive level in resistant uninoculated plants, which may represent a temporary advantage in response to the pathogen.

4.2. Homeostatic Control as a Dynamic Regulation Mechanism for Energy and Redox Status in Response to Botrytis fabae

Enhanced photosystem II (PSII) functionality at the early stages of pathogen infection may be responsible for the increased sugar production required to strengthen the response by inducing defense genes [27,62]. However, *B. cinerea* has been reported to use large amounts of soluble sugars to grow on tomato leaves [63].

Nonphotochemical chlorophyll fluorescence quenching (NPQ) is the key photoprotective process used by plants to dissipate excess light energy as heat and preserve photosynthesis as a result [64–67]. A substantial increase in NPQ was observed in tomato leaflets up to 6 h after application of a *B. cinerea* spore suspension; the increase, however, was followed by a decrease down to control levels [27]. This outcome suggests an imbalance between energy supply and demand, resulting in increased ROS production similarly as in photoinhibition, causing damage in chloroplast and eventual cell death (necrosis) [68].

On physiological grounds, Clp and FtsH proteases are believed to play major roles in chloroplast protein homeostasis. Thus, FtsH (filamentation temperature sensitive H) proteases are membrane-bound ATP-dependent zinc metalloproteases involved in the biogenesis of thylakoid membranes and quality control in the PSII repair cycle [69]. ROS production and PSII photodamage are linked to the high turnover rate of the D1 reaction center protein, which is degraded and replaced with *de novo* synthesized protein in the so-called "PSII repair cycle" [70]. FtsH proteases are among the many components mediating coordinated turnover in D1. In addition, there is evidence that programmed inhibition of the PSII repair cycle through specific downregulation of protease activity may provide plants with a mechanism to elicit ROS production and cell death upon infection [71].

In parallel to the recognition of ROS as key signaling molecules, antioxidant enzymes and ROS scavenging, scientists have accepted their potential involvement in fine-tuning defense reactions. In chloroplasts, the antioxidants ascorbate and glutathione contribute chemically to ROS quenching. In addition, H_2O_2 can be detoxified by ascorbate peroxidases (APX), peroxiredoxine (PRX) or glutathione peroxidase (GPX), reviewed in [72], as confirmed by a study on *Gentiana triflora* which suggested that PRXQ plays a role in mediating responses against the necrotrophic fungus *B. cinerea* [73].

The proteomic analysis conducted in this work revealed that three proteins identified as chloroplastic cell division protease FtsH, and a zinc dependent protease/FTSH protease 8, were highly represented in the susceptible genotype in response to *B. fabae* inoculation. The same proteins were better represented constitutively in the resistant genotype in the first sampling. In addition, a monodehydroascorbate reductase I, an L-ascorbate peroxidase

and a thioredoxin peroxidase were also better represented in both genotypes in response to inoculation in the first sampling. Zymogram analysis confirmed the results of the MS analysis, where differences in the activity bands at the molecular weights of the proteins identified by 2DE-MS were observed. In addition, inoculated and uninoculated plants of the resistant genotype exhibited some activity bands at very high molecular weights (140–250 kDa) that were not clearly observed in the susceptible genotype. This result can be ascribed to differences in the experimental conditions, which were native in the zymograms and denaturing in the 2DE-MS analysis.

Consistent with the results obtained in this work, a recent study on tomato plants revealed H_2O_2 production and enhanced photosystem II functionality 30 min after *B. cinerea* inoculation. The effect, which lasted 4 h, was suggestive of a tolerant response; however, increasing the length of exposure led to plant damage [27] by fully inhibiting PSII functionality at the application spot and nearby. This was probably a time-dependent hormetic response, suggesting a positive biological response whose effect might be reversed upon extended exposure [27,67].

5. Conclusions

Based on the proteins identified in this study (Clp and Hsp70, together with FstH proteases and ROS proteins) and their increased levels upon inoculation with *B. fabae*, a signaling response mechanism based on ROS production in the chloroplast may be elicited by the fungus. This mechanism appears to be harmful to PSII in the susceptible genotype by effect of its being associated with lengthy exposures to high ROS levels. The differential response of the two genotypes can be ascribed to a metabolic imbalance in the susceptible genotype not observed in the resistant genotype and confirming that the latter retains normal metabolism under stress. On the other hand, there is evidence that the two genotypes differ in chloroplast detoxification system, the resistant genotype exhibiting a more efficient PSII repair mechanism at the early stages of infection. Further research is required in any case to ascertain whether the ROS dose or exposure time (hormesis) is associated with the differential *V. faba* phenotypes.

Supplementary Materials: The following are available online at https://www.mdpi.com/article/10.3390/agronomy11112247/s1, Figure S1: Coomassie-stained 2DE gels images of all experimental conditions throughout the experiment: susceptible (S) and resistant (R) genotypes; control (C) and *B. fabae* inoculated (I); 6 hpi (T1) and 12 hpi (T2) and three repetitions (R1-R3), Figure S2: Chocolate spot disease severity (DS) values in the genotypes Baraca and BPL710, 2 and 6 days after *B. fabae* inoculation, Figure S3: Location of 102 identified protein spots on a virtual 2DE gel. (a) Representative Coomassie stained 2DE gel of the susceptible (left) and the resistant (right) genotypes, (b) Figure S4: Zymographic detection of proteases in faba bean leaves separated by SDS-PAGE bearing gelatin under nondenaturing conditions, control (A) and *B. fabae*-inoculated (B). Susceptible (S) and resistant genotype (R); 6 hpi (1) and 12 hpi (2). Numbers following dashes designate the particular replicates, Figure S5: Quantification of the area of protease activity bands detected by zymogram analysis corresponding to the molecular weights 40, 70, 90, 100, 140 and 250 kDa, Table S1: Dataset of the 224 protein spots detected by PDQuest image analysis.

Author Contributions: Conceptualization, M.Á.C., Á.M.V.-F. and D.R.; methodology, M.Á.C., Á.M.V.-F. and T.H.-L.; software, M.Á.C.; validation, T.H.-L. and M.Á.C.; formal analysis, M.Á.C.; investigation, M.Á.C., Á.M.V.-F. and T.H.-L.; writing—original draft preparation, M.Á.C.; writing—review and editing, M.Á.C. and Á.M.V.-F.; supervision, M.Á.C., Á.M.V.-F. and D.R.; funding acquisition, D.R. All authors have read and agreed to the published version of the manuscript.

Funding: This research was funded by Spain's Agencia Estatal de Investigación (AEI) (Grant PRIMA-DiVicia-PCI2020-111974).

Institutional Review Board Statement: Not applicable.

Informed Consent Statement: Not applicable.

Data Availability Statement: Raw data supporting reported results can be found in Supplementary Materials.

Acknowledgments: M.Á.C. is grateful to the Spanish Ministry of Science, Innovation and Universities for award of a Ramón y Cajal contract (RYC-2017-23706), and so is T.H.-L. to the University of Cordoba (Spain) for the contract under Project RYC-2017-23706.

Conflicts of Interest: The authors declare no conflict of interest.

References

1. Khazaei, H.; O'Sullivan, D.M.; Stoddard, F.L.; Adhikari, K.N.; Paull, J.G.; Schulman, A.H.; Andersen, S.U.; Vandenberg, A. Recent advances in faba bean genetic and genomic tools for crop improvement. *Legum. Sci.* **2021**, *3*, e75. [CrossRef]
2. Rispail, N.; Kaló, P.; Kiss, G.B.; Ellis, T.N.; Gallardo, K.; Thompson, R.D.; Prats, E.; Larrainzar, E.; Ladrera, R.; González, E.M.; et al. Model legumes contribute to faba bean breeding. *Field Crop. Res.* **2010**, *115*, 253–269. [CrossRef]
3. Cernay, C.; Ben-Ari, T.; Pelzer, E.; Meynard, J.-M.; Makowski, D. Estimating variability in grain legume yields across Europe and the Americas. *Sci. Rep.* **2015**, *5*, 11171. [CrossRef]
4. Kharrat, M.; Le Guen, J.; Tivoli, B. Genetics of resistance to 3 isolates of *Ascochyta fabae* on Faba bean (*Vicia faba* L.) in controlled conditions. *Euphytica* **2006**, *151*, 49–61. [CrossRef]
5. Tivoli, B.; Baranger, A.; Avila, C.; Banniza, S.; Barbetti, M.; Chen, W.; Davidson, J.; Lindeck, K.; Kharrat, M.; Rubiales, D.; et al. Screening techniques and sources of resistance to foliar diseases caused by major necrotrophic fungi in grain legumes. *Euphytica* **2006**, *147*, 223–253. [CrossRef]
6. Stoddard, F.; Nicholas, A.; Rubiales, D.; Thomas, J.; Villegas-Fernández, A. Integrated pest management in faba bean. *Field Crop. Res.* **2010**, *115*, 308–318. [CrossRef]
7. Harrison, J.G. Effects of environmental factors on growth of lesions on field bean leaves infected by *Botrytis fabae*. *Ann. Appl. Biol.* **1980**, *95*, 53–61. [CrossRef]
8. Harrison, J.G. The biology of *Botrytis* spp. on *Vicia* beans and chocolate spot disease—A review. *Plant Pathol.* **1988**, *37*, 168–201. [CrossRef]
9. Murray, G.M.; Brennan, J.P. *The Current and Potential Costs from Diseases of Pulse Crops in Australia*; Grains Research and Development Corporation: Canberra, Australia, 2012.
10. Villegas-Fernández, A.; Sillero, J.; Emeran, A.; Winkler, J.; Raffiot, B.; Tay, J.; Flores, F.; Rubiales, D. Identification and multi-environment validation of resistance to *Botrytis fabae* in *Vicia faba*. *Field Crop. Res.* **2009**, *114*, 84–90. [CrossRef]
11. Sillero, J.C.; Villegas-Fernández, A.M.; Thomas, J.; Rojas-Molina, M.M.; Emeran, A.A.; Fernández-Aparicio, M.; Rubiales, D. Faba bean breeding for disease resistance. *Field Crop. Res.* **2010**, *115*, 297–307. [CrossRef]
12. Bouhassan, A.; Sadiki, M.; Tivoli, B. Evaluation of a collection of faba bean (*Vicia faba* L.) genotypes originating from the Maghreb for resistance to chocolate spot (*Botrytis fabae*) by assessment in the field and laboratory. *Euphytica* **2004**, *135*, 55–62. [CrossRef]
13. Williamson, B.; Tudzynski, B.; Tudzynski, P.; van Kan, J.A. *Botrytis cinerea*: The cause of grey mould disease. *Mol. Plant Pathol.* **2007**, *8*, 561–580. [CrossRef] [PubMed]
14. Cimmino, A.; Villegas-Fernández, A.M.; Andolfi, A.; Melck, D.; Rubiales, D.; Evidente, A. Botrytone, a New Naphthalenone Pentaketide Produced by *Botrytis fabae*, the Causal Agent of Chocolate Spot Disease on *Vicia faba*. *J. Agric. Food Chem.* **2011**, *59*, 9201–9206. [CrossRef] [PubMed]
15. AbuQamar, S.F.; Moustafa, K.; Tran, L.S.P. 'Omics' and plant responses to *Botrytis cinerea*. *Front. Plant. Sci.* **2016**, *7*, 1658. [CrossRef] [PubMed]
16. Ren, H.; Bai, M.; Sun, J.; Liu, J.; Ren, M.; Dong, Y.; Wang, N.; Ning, G.; Wang, C. RcMYB84 and RcMYB123 mediate jasmonate-induced defense responses against *Botrytis cinerea* in rose (*Rosa chinensis*). *Plant. J.* **2020**, *103*, 1839–1849. [CrossRef] [PubMed]
17. AbuQamar, S.; Ajeb, S.; Sham, A.; Enan, M.R.; Iratni, R. A mutation in the expansin-like A2 gene enhances resistance to necrotrophic fungi and hypersensitivity to abiotic stress in *Arabidopsis thaliana*. *Mol. Plant. Pathol.* **2013**, *14*, 813–827. [CrossRef] [PubMed]
18. AbuQamar, S. Expansins: Cell Wall Remodeling Proteins with a Potential Function in Plant Defense. *J. Plant Biochem. Physiol.* **2014**, *2*, 118. [CrossRef]
19. VanEtten, H.D.; Mansfield, J.W.; Bailey, J.A.; Farmer, E.E. Two Classes of Plant Antibiotics: Phytoalexins versus 'Phytoanticipins'. *Plant Cell* **1994**, *6*, 1191. [CrossRef]
20. VAN Loon, L.; VAN Strien, E. The families of pathogenesis-related proteins, their activities, and comparative analysis of PR-1 type proteins. *Physiol. Mol. Plant Pathol.* **1999**, *55*, 85–97. [CrossRef]
21. van Loon, L.; Rep, M.; Pieterse, C. Significance of Inducible Defense-related Proteins in Infected Plants. *Annu. Rev. Phytopathol.* **2006**, *44*, 135–162. [CrossRef] [PubMed]
22. Dangl, J.L.; Jones, J.D.G. Plant pathogens and integrated defence responses to infection. *Nature* **2001**, *411*, 826–833. [CrossRef] [PubMed]
23. Colmenares, A.J.; Aleu, J.; Duran-Patron, R.M.; Collado, I.G.; Hernandez-Galán, R. The putative role of botrydial and related metabolites in the infection mechanism of *Botrytis cinerea*. *J. Chem. Ecol.* **2002**, *28*, 997–1005. [CrossRef] [PubMed]

24. Patykowski, J.; Urbanek, H. Activity of Enzymes Related to H_2O_2 Generation and Metabolism in Leaf Apoplastic Fraction of Tomato Leaves Infected with *Botrytis cinerea*. *J. Phytopathol.* **2003**, *151*, 153–161. [CrossRef]
25. Rolke, Y.; Liu, S.; Quidde, T.; Williamson, B.; Schouten, A.; Weltring, K.-M.; Siewers, V.; Tenberge, K.B.; Tudzynski, B.; Tudzynski, P. Functional analysis of H2O2-generating systems in *Botrytis cinerea*: The major Cu-Zn-superoxide dismutase (BCSOD1) contributes to virulence on French bean, whereas a glucose oxidase (BCGOD1) is dispensable. *Mol. Plant Pathol.* **2004**, *5*, 17–27. [CrossRef]
26. Hua, L.; Yong, C.; Zhanquan, Z.; Boqiang, L.; Guozheng, Q.; Shiping, T. Pathogenic mechanisms and control strategies of *Botrytis cinerea* causing post-harvest decay in fruits and vegetables. *Food Qual. Saf.* **2018**, *2*, 111–119. [CrossRef]
27. Stamelou, M.-L.; Sperdouli, I.; Pyrri, I.; Adamakis, I.-D.; Moustakas, M. Hormetic Responses of Photosystem II in Tomato to *Botrytis cinerea*. *Plants* **2021**, *10*, 521. [CrossRef]
28. El-Komy, M.H. Comparative Analysis of Defense Responses in Chocolate Spot-Resistant and -Susceptible Faba Bean (*Vicia faba*) Cultivars Following Infection by the Necrotrophic Fungus *Botrytis fabae*. *Plant Pathol. J.* **2014**, *30*, 355–366. [CrossRef]
29. Villegas-Fernández, Á.M.; Krajinski, F.; Schlereth, A.; Madrid, E.; Rubiales, D. Characterization of Transcription Factors Following Expression Profiling of *Medicago truncatula—Botrytis* spp. Interactions. *Plant Mol. Biol. Rep.* **2014**, *32*, 1030–1040. [CrossRef]
30. Birkenbihl, R.P.; Diezel, C.; Somssich, I.E. Arabidopsis WRKY33 Is a Key Transcriptional Regulator of Hormonal and Metabolic Responses toward *Botrytis cinerea* Infection. *Plant Physiol.* **2012**, *159*, 266–285. [CrossRef]
31. Windram, O.; Madhou, P.; McHattie, S.; Hill, C.; Hickman, R.; Cooke, E.; Jenkins, D.J.; Penfold, C.A.; Baxter, L.; Breeze, E.; et al. *Arabidopsis* Defense against *Botrytis cinerea*: Chronology and Regulation Deciphered by High-Resolution Temporal Transcriptomic Analysis. *Plant Cell* **2012**, *24*, 3530–3557. [CrossRef]
32. Marra, R.; Ambrosino, P.; Carbone, V.; Vinale, F.; Woo, S.L.; Ruocco, M.; Ciliento, R.; Lanzuise, S.; Ferraioli, S.; Soriente, I.; et al. Study of the three-way interaction between *Trichoderma atroviride*, plant and fungal pathogens by using a proteomic approach. *Curr. Genet.* **2006**, *50*, 307–321. [CrossRef] [PubMed]
33. Shah, P.; Powell, A.L.; Orlando, R.; Bergmann, C.; Gutierrez-Sanchez, G. Proteomic Analysis of Ripening Tomato Fruit Infected by *Botrytis cinerea*. *J. Proteome Res.* **2012**, *11*, 2178–2192. [CrossRef] [PubMed]
34. Mokhtar, M.M.; Hussein, E.H.A.; El-Assal, S.E.-D.S.; Atia, M.A.M. VfODB: A comprehensive database of ESTs, EST-SSRs, mtSSRs, microRNA-target markers and genetic maps in *Vicia faba*. *AoB Plants* **2020**, *12*, plaa064. [CrossRef]
35. Villegas-Fernández, A.M.; Sillero, J.C.; Rubiales, D. Screening faba bean for chocolate spot resistance: Evaluation methods and effects of age of host tissue and temperature. *Eur. J. Plant Pathol.* **2011**, *132*, 443–453. [CrossRef]
36. Wang, W.; Vignani, R.; Scali, M.; Cresti, M. A universal and rapid protocol for protein extraction from recalcitrant plant tissues for proteomic analysis. *Electrophoresis* **2006**, *27*, 2782–2786. [CrossRef] [PubMed]
37. Castillejo, M.A.; Bani, M.; Rubiales, D. Understanding pea resistance mechanisms in response to *Fusarium oxysporum* through proteomic analysis. *Phytochemistry* **2015**, *115*, 44–58. [CrossRef]
38. Mathesius, U.; Keijzers, G.; Natera, S.H.A.; Weinman, J.J.; Djordjevic, M.A.; Rolfe, B.G. Establishment of a root proteome reference map for the model legume *Medicago truncatula* using the expressed sequence tag database for peptide mass fingerprinting. *Proteomics* **2001**, *1*, 1424–1440. [CrossRef]
39. Sharov, A.A.; Dudekula, D.; Ko, M.S.H. A web-based tool for principal component and significance analysis of microarray data. *Bioinformatics* **2005**, *21*, 2548–2549. [CrossRef]
40. Shevchenko, A.; Wilm, M.; Vorm, O.; Mann, M. Mass Spectrometric Sequencing of Proteins from Silver-Stained Polyacrylamide Gels. *Anal. Chem.* **1996**, *68*, 850–858. [CrossRef]
41. Bradford, M.M. A rapid and sensitive method for the quantitation of microgram quantities of protein utilizing the principle of protein-dye binding. *Anal. Biochem.* **1976**, *7*, 248–254. [CrossRef]
42. Heussen, C.; Dowdle, E.B. Electrophoretic analysis of plasminogen activators in polyacrylamide gels containing sodium dodecyl sulfate and copolymerized substrates. *Anal. Biochem.* **1980**, *102*, 196–202. [CrossRef]
43. Neuhoff, V.; Arold, N.; Taube, D.; Ehrhardt, W. Improved staining of proteins in polyacrylamide gels including isoelectric focusing gels with clear background at nanogram sensitivity using Coomassie Brilliant Blue G-250 and R-250. *Electrophoresis* **1988**, *9*, 255–262. [CrossRef] [PubMed]
44. Torres, M.A.; Dangl, J.L. Functions of the respiratory burst oxidase in biotic interactions, abiotic stress and development. *Curr. Opin. Plant Biol.* **2005**, *8*, 397–403. [CrossRef]
45. Karpinski, S.; Reynolds, H.; Karpinska, B.; Wingsle, G.; Creissen, G.; Mullineaux, P. Systemic Signaling and Acclimation in Response to Excess Excitation Energy in *Arabidopsis*. *Science* **1999**, *284*, 654–657. [CrossRef]
46. Vandenabeele, S.; Vanderauwera, S.; Vuylsteke, M.; Rombauts, S.; Langebartels, C.; Seidlitz, H.K.; Zabeau, M.; Van Montagu, M.; Inzé, D.; Van Breusegem, F. Catalase deficiency drastically affects gene expression induced by high light in *Arabidopsis thaliana*. *Plant J.* **2004**, *39*, 45–58. [CrossRef]
47. Laloi, C.; Stachowiak, M.; Pers-Kamczyc, E.; Warzych, E.; Murgia, I.; Apel, K. Cross-talk between singlet oxygen- and hydrogen peroxide-dependent signaling of stress responses in *Arabidopsis thaliana*. *Proc. Natl. Acad. Sci. USA* **2007**, *104*, 672–677. [CrossRef] [PubMed]
48. Joo, J.H.; Wang, S.; Chen, J.G.; Jones, A.M.; Fedoroff, N.V. Different signaling and cell death roles of heterotrimeric G protein alpha and beta subunits in the *Arabidopsis* oxidative stress response to ozone. *Plant Cell* **2005**, *17*, 957–970. [CrossRef]
49. Belhaj, K.; Lin, B.; Mauch, F. The chloroplast protein RPH1 plays a role in the immune response of *Arabidopsis* to *Phytophthora brassicae*. *Plant J.* **2009**, *58*, 287–298. [CrossRef]

50. Kuźniak, E.; Świercz, U.; Chojak-Koźniewska, J.; Sekulska-Nalewajko, J.; Gocławski, J. Automated image analysis for quantification of histochemical detection of reactive oxygen species and necrotic infection symptoms in plant leaves. *J. Plant Interact.* **2014**, *9*, 167–174. [CrossRef]
51. Nishiyama, Y.; Yamamoto, H.; Allakhverdiev, S.; Inaba, M.; Yokota, A.; Murata, N. Oxidative stress inhibits the repair of photodamage to the photosynthetic machinery. *EMBO J.* **2001**, *20*, 5587–5594. [CrossRef]
52. Meng, L.; Höfte, M.; Van Labeke, M.-C. Leaf age and light quality influence the basal resistance against *Botrytis cinerea* in strawberry leaves. *Environ. Exp. Bot.* **2019**, *157*, 35–45. [CrossRef]
53. Li, Z.; Wakao, S.; Fischer, B.B.; Niyogi, K.K. Sensing and Responding to Excess Light. *Annu. Rev. Plant Biol.* **2009**, *60*, 239–260. [CrossRef]
54. Gawroński, P.; Burdiak, P.; Scharff, L.B.; Mielecki, J.; Górecka, M.; Zaborowska, M.; Leister, D.; Waszczak, C.; Karpiński, S. CIA2 and CIA2-LIKE are required for optimal photosynthesis and stress responses in *Arabidopsis thaliana*. *Plant J.* **2021**, *105*, 619–638. [CrossRef]
55. Pulido, P.; Llamas, E.; Rodriguez-Concepcion, M. Both Hsp70 chaperone and Clp protease plastidial systems are required for protection against oxidative stress. *Plant Signal. Behav.* **2017**, *12*, e1290039. [CrossRef] [PubMed]
56. Muthusamy, S.K.; Dalal, M.; Chinnusamy, V.; Bansal, K.C. Differential Regulation of Genes Coding for Organelle and Cytosolic ClpATPases under Biotic and Abiotic Stresses in Wheat. *Front. Plant Sci.* **2016**, *7*, 929. [CrossRef]
57. Doyle, S.M.; Wickner, S. Hsp104 and ClpB: Protein disaggregating machines. *Trends Biochem. Sci.* **2009**, *34*, 40–48. [CrossRef]
58. Park, S.; Rodermel, S.R. Mutations in ClpC2/Hsp100 suppress the requirement for FtsH in thylakoid membrane biogenesis. *Proc. Natl. Acad. Sci. USA* **2004**, *101*, 12765–12770. [CrossRef] [PubMed]
59. Sjögren, L.L.; MacDonald, T.M.; Sutinen, S.; Clarke, A.K. Inactivation of the clpC1 Gene Encoding a Chloroplast Hsp100 Molecular Chaperone Causes Growth Retardation, Leaf Chlorosis, Lower Photosynthetic Activity, and a Specific Reduction in Photosystem Content. *Plant Physiol.* **2004**, *136*, 4114–4126. [CrossRef] [PubMed]
60. Adam, Z.; Rudella, A.; van Wijk, K.J. Recent advances in the study of Clp, FtsH and other proteases located in chloroplasts. *Curr. Opin. Plant Biol.* **2006**, *9*, 234–240. [CrossRef] [PubMed]
61. Wu, H.; Ji, Y.; Du, J.; Kong, D.; Liang, H.; Ling, H.-Q. ClpC1, an ATP-dependent Clp protease in plastids, is involved in iron homeostasis in *Arabidopsis* leaves. *Ann. Bot.* **2010**, *105*, 823–833. [CrossRef] [PubMed]
62. Moghaddam, M.R.B.; Van Den Ende, W. Sugars and plant innate immunity. *J. Exp. Bot.* **2012**, *63*, 3989–3998. [CrossRef]
63. Courbier, S.; Grevink, S.; Sluijs, E.; Bonhomme, P.; Kajala, K.; Van Wees, S.C.M.; Pierik, R. Far-red light promotes *Botrytis cinerea* disease development in tomato leaves via jasmonate-dependent modulation of soluble sugars. *Plant Cell Environ.* **2020**, *43*, 2769–2781. [CrossRef]
64. Moustaka, J.; Moustakas, M. Photoprotective mechanism of the non-target organism *Arabidopsis thaliana* to paraquat exposure. *Pestic. Biochem. Physiol.* **2014**, *111*, 1–6. [CrossRef] [PubMed]
65. Moustaka, J.; Tanou, G.; Adamakis, I.-D.; Eleftheriou, E.P.; Moustakas, M. Leaf Age-Dependent Photoprotective and Antioxidative Response Mechanisms to Paraquat-Induced Oxidative Stress in *Arabidopsis thaliana*. *Int. J. Mol. Sci.* **2015**, *16*, 13989–14006. [CrossRef] [PubMed]
66. Ruban, A.V. Nonphotochemical Chlorophyll Fluorescence Quenching: Mechanism and Effectiveness in Protecting Plants from Photodamage. *Plant Physiol.* **2016**, *170*, 1903–1916. [CrossRef] [PubMed]
67. Agathokleous, E.; Kitao, M.; Harayama, H. On the Nonmonotonic, Hormetic Photoprotective Response of Plants to Stress. *Dose-Response* **2019**, *17*, 1559325819838420. [CrossRef]
68. Sperdouli, I.; Moustakas, M. A better energy allocation of absorbed light in photosystem II and less photooxidative damage contribute to acclimation of *Arabidopsis thaliana* young leaves to water deficit. *J. Plant Physiol.* **2014**, *171*, 587–593. [CrossRef]
69. Kato, Y.; Sakamoto, W. FtsH Protease in the Thylakoid Membrane: Physiological Functions and the Regulation of Protease Activity. *Front. Plant Sci.* **2018**, *9*, 855. [CrossRef]
70. Mulo, P.; Sirpiö, S.; Suorsa, M.; Aro, E.-M. Auxiliary proteins involved in the assembly and sustenance of photosystem II. *Photosynth. Res.* **2008**, *98*, 489–501. [CrossRef]
71. Seo, S.; Okamoto, M.; Iwai, T.; Iwano, M.; Fukui, K.; Isogai, A.; Nakajima, N.; Ohashi, Y. Reduced Levels of Chloroplast FtsH Protein in Tobacco Mosaic Virus–Infected Tobacco Leaves Accelerate the Hypersensitive Reaction. *Plant Cell* **2000**, *12*, 917–932.
72. Kangasjärvi, S.; Neukermans, J.; Li, S.; Aro, E.-M.; Noctor, G. Photosynthesis, photorespiration, and light signalling in defence responses. *J. Exp. Bot.* **2012**, *63*, 1619–1636. [CrossRef] [PubMed]
73. Kiba, A.; Nishihara, M.; Tsukatani, N.; Nakatsuka, T.; Kato, Y.; Yamamura, S. A Peroxiredoxin Q Homolog from Gentians is Involved in Both Resistance against Fungal Disease and Oxidative Stress. *Plant Cell Physiol.* **2005**, *46*, 1007–1015. [CrossRef] [PubMed]